ACS APPLIED NANO MATERIALS

Article

Cite This: ACS Appl. Nano Mater. 2019, 2, 7362−7371

www.acsanm.org

Femtosecond-Laser-Produced Underwater "Superpolymphobic" Nanorippled Surfaces: Repelling Liquid Polymers in Water for Applications of Controlling Polymer Shape and Adhesion

Jiale Yong,[†,‡] Subhash C. Singh,[†] Zhibing Zhan,[†] Mohamed EIKabbash,[†] Feng Chen,*[,‡] and Chunlei Guo*[,†]

[†]The Institute of Optics, University of Rochester, Rochester, New York 14627, United States

[‡]Shaanxi Key Laboratory of Photonics Technology for Information, School of Electronics & Information Engineering, Xi'an Jiaotong University, Xi'an 710049, P. R. China

Supporting Information

ABSTRACT: A femtosecond (fs)-laser-processed surface that repels liquid polymer in water is reported in this paper. We define this phenomenon as the "superpolymphobicity". Three-level microstructures (including microgrooves, micromountains/microholes between the microgrooves, and nanoripples on the whole surface) were directly created on the stainless steel surface via fs laser processing. A liquid polydimethylsiloxane (PDMS) droplet on the textured surface had the contact angle of 156 ± 3° and contact angle hysteresis less than 4° in water, indicating excellent underwater superpolymphobicity of the fs-laser-induced hierarchical microstructures. The contact between the resultant superhydrophilic hierarchical microstructures and the submerged liquid PDMS droplet is verified at the underwater Cassie state. The underwater superpolymphobicity enables to design the shape of cured PDMS and selectively avoid the adhesion at the PDMS/substrate interface, different from the previously reported superwettabilities. As the examples, the microlens array and microfluidics system were prepared based on the laser-induced underwater superpolymphobic microstructures.

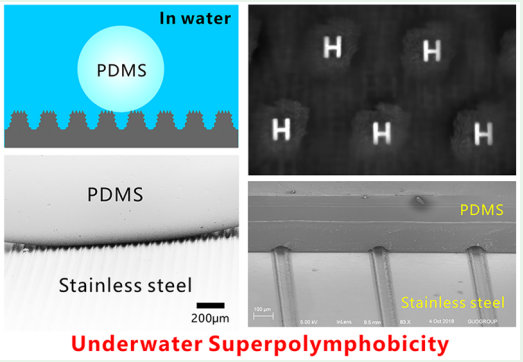

KEYWORDS: *underwater superpolymphobicity, femtosecond laser, polymer repellence, three-level microstructure, superhydrophilicity*

1. INTRODUCTION

Surface wettability depending on the molecular interaction at the interface of solid, liquid, and gas phases plays an important role in the animals and plants' survival and in our daily life. Materials with various superwettabilities (e.g. superhydrophobicity and superoleophobicity) attract increasing interest due to their rich practical applications in antiliquids,[1] self-cleaning coating,[2,3] anti-icing/fogging/snowing,[4,5] manipulation of liquid droplets,[6,7] oil/water separation,[8−10] antifouling,[11] anticorrosion,[12] drag reduction,[13] lab chip,[14,15] cell engineering,[16,17] water harvesting,[18] microfluidics,[19,20] buoyancy enhancement,[21] liquid patterning,[22] and so on. Illumined by superwettability in nature, vast array of superhydrophobic and superoleophobic materials have been artificially fabricated in the past two decades.[1,23−26] However, superhydrophobic/superoleophobic surfaces just repel pure water solution and oil. On the other hand, polymers are widely used in chemical industry, food processing, building, bioengineering, agriculture, pharmaceutical industry, and so on. Some polymers have their corresponding liquid state; for example, polydimethylsiloxane (PDMS) is generally prepared from mixing a prepolymer and a curing agent.[27,28] The uncured PDMS is in a liquid phase, and its shape is fixed after curing at high temperature due to the cross-linking-induced solidification.

Preventing liquid polymer from adhering to a solid surface and fixing the configuration of the cured polymer remain problematic for the applications related to polymers, such as polymer production, polymer casting manufacturing, and 3D printing technology. Liquid polymers have complex composition, higher viscosity, and lower fluidity in comparison to water and oils. Surprisingly, research on the wettability of liquid polymers on a solid substrate has still not been reported until now.[1,18−22] Controlling the wetting property of liquid polymers can significantly reduce the adhesion between substrates and polymers and enable to design the shapes of cured polymers.

Similar to the etymology of the terms "superhydrophobicity" and "superoleophobicity" in the field of wettability ("hydro" and "phobic" come from the Greek words, meaning "water" and "fear", respectively; "oleo" comes from the Latin for "oils or fats"),[1,29] here we use the newly coined word "super-

Received: September 26, 2019
Accepted: October 25, 2019
Published: October 25, 2019

DOI: 10.1021/acsanm.9b01869
ACS Appl. Nano Mater. 2019, 2, 7362−7371

polymphobicity" ("polym" is an abbreviation of polymer) to describe the phenomenon that a solid surface greatly repels liquid polymers with the contact angle (CA) of polymer droplet higher than 150° and has very low polymer adhesion. Superpolymphobicity significantly differs from the superwetting states for water and oils. Establishing the principle for achieving superpolymphobicity has very important significance, and the preparation and application of superpolymphobic surfaces are considerable challenges.

In this paper, hierarchical microstructure was created on the surface of stainless steel substrate by single-step femtosecond (fs) laser processing. When the as-prepared nanorippled surface is dipped into water, the liquid PDMS droplet is strongly repelled by the laser-induced microstructure, indicating excellent underwater superpolymphobicity of the rough microstructure. The contact of the PDMS droplet on the textured surface is at the underwater Cassie wetting state which is verified by the transmission optical photographs and scanning electronic microscope (SEM) images. We show that the underwater superpolymphobic microstructure can be used to design the shape of the cured PDMS and selectively avoid the adhesion at the PDMS/substrate interface. As a result, a simple microlens array and a microfluidics system were prepared.

2. RESULTS AND DISCUSSION

A fs laser is widely applied in controlling the wettability of a solid substrate. For example, Mazur et al.[30] and Stratakis et al.[31] used the fs laser to create superhydrophobic silicon microstructures under the SF_6 gas. The laser-structured surface, named black silicon, is completely covered by uniform microscale conical spikes with abundant nanoscale protrusions. After fluoroalkylsilane modification, the resultant surface showed excellent superhydrophobicity and very low water adhesion. Chen et al. developed the method for constructing superhydrophobic Si surfaces by simple fs laser treatment in an ambient environment.[32−35] Yong et al. obtained underwater superoleophobicity and underwater superaerophobicity on the Si surfaces with micromountain array structures which were produced by the fs laser.[36,37] Inspired by nepenthes, Yong et al. also developed a method to fabricate a slippery liquid infused porous surface (SLIPS) by using fs laser treating polymer surfaces.[38,39] The as-prepared SLIPS exhibits excellent liquid-repellent ability to a broad range of liquids.

Hierarchical microstructures were generated on the stainless steel surface via fs laser processing. As depicted in Figure 1a, the sample was mounted on a translation platform. By using a plano-convex lens (focal length of 25 cm), the fs laser was focused on the surface of stainless steel sheet. Line-by-line laser scanning was used to ablate the sample surface (Figure 1b). The power of the adopted laser beam was set constantly at 500 mW, and the laser scanning speed was 2.5 mm s^{-1}. The interval (Λ) of the laser scanning lines was controlled by the program. To investigate the underwater polymer wettability of the laser-treated stainless steel surface, the PDMS (Figure 1d) was adopted as the tested liquid polymer. The liquid PDMS was a mixture of prepolymer and curing agent, without curing. The stainless steel sample was first immersed in water, and then a microsyringe was plugged into water and dispensed a liquid PDMS droplet with rich $-CH_3$ groups on the sample surface (Figure 1e).

Binary microstructure plays an important role in forming the superhydrophobicity for lotus leaves and the underwater

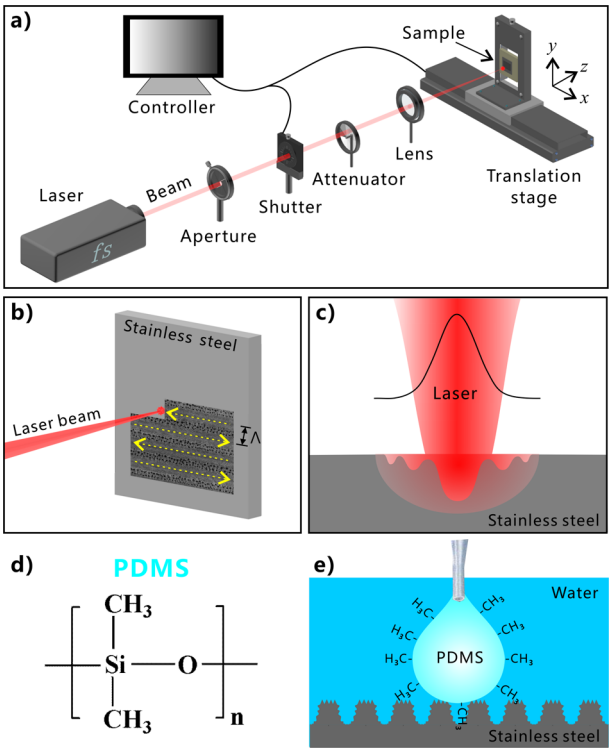

Figure 1. Schematic of treating stainless steel surface via the focused fs laser and the test of underwater polymer wettability. (a) Experimental setup. (b) Schematic illustration of line-by-line scanning process. (c) Interaction between focused fs laser beam and stainless steel substrate. (d) Chemical structure of the PDMS component. (e) Dripping a liquid PDMS droplet onto the stainless steel surface in water.

superoleophobicity for fish scales.[40,41] Interestingly, a kind of three-level microstructure can be directly prepared on stainless steel surface through one-step fs laser processing. The track of the laser ablating line turns to a single microscale groove. By use of the large-space line-by-line scanning technique, an array of microgrooves was created on the sample surface, as shown in Figure 2a,b,d. The period of the microgrooves array is determined by Λ (e.g., Λ = 80 μm in Figure 2). The resultant grooves have a width of ∼46.2 μm and a depth of ∼13.4 μm (Figure S1, Supporting Information). The bottom of every microgroove is covered with periodic nanoscale ripples, i.e., the so-called laser-induced periodic surface structure (LIPSS) (Figure 2e,h).[42,43] The width of the nanoripples is only ∼352 nm, and their height is in a range of tens to hundreds of nanometers. Ridges between the adjacent microgrooves were formed (Figure 2b,d,e) which are composed of random mountain-shaped microstructure and abundant microholes (Figure 2c,e,f,g). The diameter of the micromountains is ∼5.2−11.7 μm, and their height reaches up to 27.5 μm. Every micromountain is surrounded by several deep microholes with a diameter of 2.5−9.6 μm and the maximum depth of 19.4 μm (Figure 2f and Figure S1). The top surface of the micromountains is also completely coated with LIPSS (Figure 2i). Such LIPSS has similar period and size with that on the microgrooves' bottom. In addition, the nanoripples' orientation on the micromountains is consistent with that on the microgrooves' bottom. After laser treatment, the whole structured surface is covered with nanoripples. Therefore, the laser-ablated stainless steel surface has three-level micro-

DOI: 10.1021/acsanm.9b01869
ACS Appl. Nano Mater. 2019, 2, 7362−7371

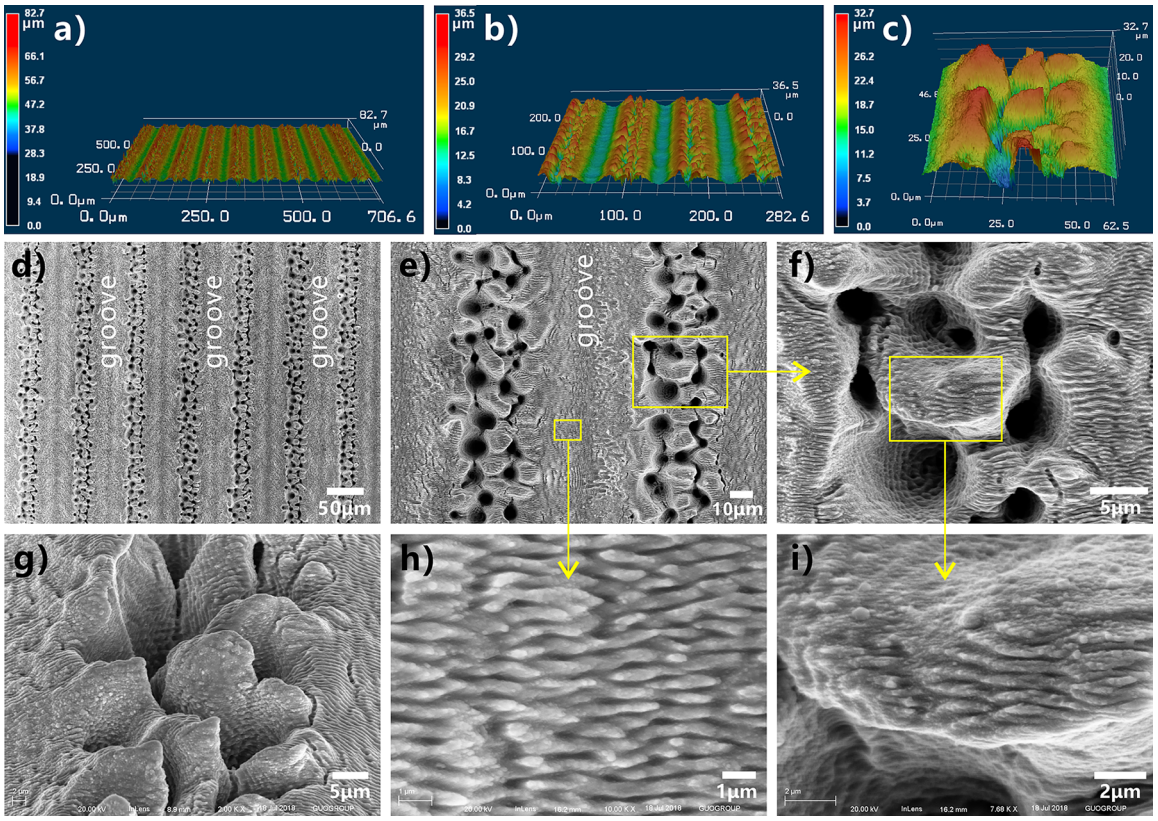

Figure 2. Surface microstructures of the stainless steel sheet after fs laser processing. (a–c) Three-dimensional (3D) morphology of the sample surface: (a) laser-structured microgrooves array, (b) high-magnification image of the microgrooves array, and (c) microstructure on the ridges. (d–i) SEM images of the sample surface: (d, e) laser-induced microgrooves array, (f) ridge structure between the adjacent microgrooves, (g) tilted-view image of a single ridge, (h) large-magnified image of the valley bottom of the microgroove, and (i) microstructure on the micromountains.

structures, including microgrooves, micromountains/microholes on the ridges between the microgrooves, and nanoripples on the micromountains.

The intensity of the fs laser is very high and at the Gauss-curved distribution. As shown in Figure 1c, the spot center has the highest laser fluence, so strong ablation occurs at the focused point. The surface materials are tempestuously removed away by laser ablation, resulting in a microgroove along every scanning line. The region near the spot has a middle fluence compared to the spot center and the spot fringe. Under repetitious impulses, the substrate material around the spot center undergoes melting due to the extreme heat, the explosion of the melted metal, cooling rapidly, and resolidification.[43] During such a series of processes, separated micromountains and microholes appear near the laser-focused point, and they finally distribute on the ridges between the center-laser-induced microgrooves. The submicrometer structure can usually be induced by the laser with low intensity. With the spot center moving forward, the low-fluence spot fringe begins to treat the material surface, and LIPSS (i.e., periodic nanoscale ripples) is induced on both the microgroove bottom and the micromountain surface. The periodic nanoripples, a typical characteristic of laser ablation, are generally believed to have developed from the interference between incident laser pulses and the scattered tangential wave caused by the previous pulses.[42,43] As a result, a three-level microstructure was created on the surface of stainless steel after fs laser treatment, which is caused by the nonuniform fluence distribution of the high-intensity laser beam and the uniform motion of the laser focused spot (Figure 1c).

The multilevel microstructure has a significant influence on the wettability of stainless steel surface, as shown in Figure 3. The original flat stainless steel surface exhibits inherent hydrophilicity in air. A water droplet on the bare flat surface has the water CA (WCA) of 79 ± 2° (Figure 3a). Similarly, a liquid PDMS droplet on such surface shows a polymer CA (PCA) of 23 ± 2° (Figure 3c); that is, the stainless steel is intrinsically "polymphilic". In general, the rough surface microstructure can amplify the original wettability of a solid surface. As long as a water droplet touched the laser-structured surface, it would quickly spread out and fully wet the ablated area, resulting in a WCA closing to zero (Figure 3b,f, and Movie S1). The result indicates the laser-induced microstructure showed superhydrophilicity. With regard to the PDMS droplet, its PCA decreased to 16 ± 3° when it was placed onto a rough surface (Figure 3d). It is noticed that the liquid PDMS is unable to completely wet the rough surface microstructures because of the high viscosity and low fluidity of the polymer liquid. When the stainless steel samples were dipped into water, their wettability to liquid PDMS droplet is entirely different from that in air. Underwater liquid PDMS droplet on the flat stainless steel substrate had a PCA of 116 ± 10° (Figure S2a) and could firmly adhere to the surface even the sample was 90° tilted (Figure S2b). In contrast, the laser-structured surface had a great repellence to liquid PDMS in a water medium. Figure 3g and Movie S2 depict the dynamic process of moving a PDMS droplet to contact and then leave the immersed rough stainless steel surface. The liquid PDMS droplet suspended on a needle nozzle was lowered slowly until the droplet had an appropriate contact with the laser-

DOI: 10.1021/acsanm.9b01869
ACS Appl. Nano Mater. 2019, 2, 7362–7371

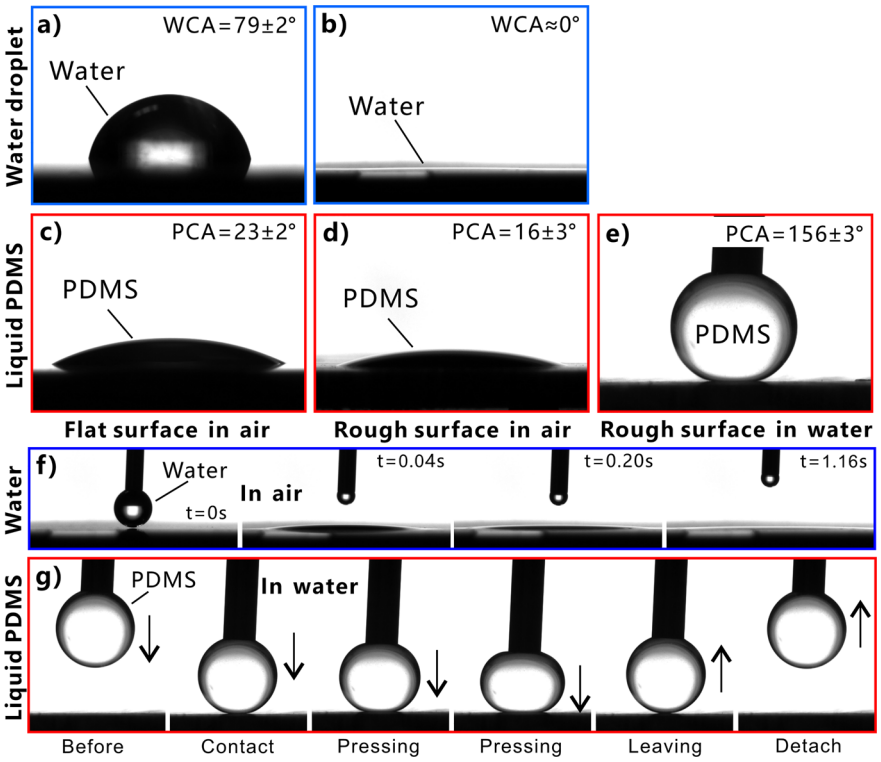

Figure 3. Surface wettability of different stainless steel surfaces. (a, b) Water droplets on (a) the original untreated surface and (b) the laser-induced rough surface in air. (c–e) Liquid PDMS droplets on (c) the in-air original untreated surface, (d) the in-air laser-induced rough surface, and (e) the underwater laser-induced rough surface. (f) Small water droplet spreading out on the laser-structured surface. (g) Moving a PDMS droplet to contact and then leave the immersed rough stainless steel surface.

structured surface. Then, the PDMS droplet was lifted up with the needle. The measured PCA was as large as 156 ± 3° for the liquid PDMS droplet on the sample surface, even after slightly pressing on the PDMS droplet (Figure 3e). The PDMS droplet could easily detach from the substrate. Upon surface detachment, the PDMS droplet maintained its spherical shape without apparent shape deformation, and no PDMS residual adhered to the stainless steel (Figure 3g). The measured CA hysteresis (CAH) of the PDMS droplet was no more than 4° on the sample surface, demonstrating ultralow adhesion between liquid PDMS and the laser-processed surface. Therefore, the laser-induced three-level microstructure has excellent underwater superpolymphobicity.

The underwater superpolymphobicity could not be achieved on the stainless steel surface if there is no laser-induced multilevel microstructure. The stainless steel substrate is inherently hydrophilic with intrinsic BCA smaller than 90°. A water droplet on the untreated flat substrate is at the Young wetting state (Figure 4a). Laser processing enables hierarchical microstructure to form on the stainless steel surface, so the actual surface area of the sample is greatly increased. For a hydrophilic substrate, the hydrophilicity can generally be enhanced by surface microstructure.[1] When a water droplet is in contact with the laser-induced microstructures, water can fully wet the microstructures whether it touches the top of the ridges or the valley of the microgrooves because of the increased surface area and capillary action (Figure 4b).[44−46] The wetting of the water droplet on the surface microstructure is at the Wenzel state.[1] The intrinsic hydrophilicity is enhanced to superhydrophilicity after laser ablation for a stainless steel sample. As the sample is submerged into water, water wets and fills in all of the microgrooves and the space between the surface microstructure (Figure 4c). The surrounding water likes being embedded in the laser-induced microstructure, which has the great ability to prevent a polymer droplet from effectively touching the sample surface by reason of the insolubility and mutual exclusion between liquid PDMS and water. When a PDMS droplet is further placed on the rough sample surface previously submerged in water, a water cushion composed of water pockets forms between PDMS and the stainless steel (Figure 4d). Because an intermolecular repulsive effect occurs between the polar molecules (water) and nonpolar molecules (liquid PDMS), the trapped water layer in the hierarchical surface microstructure provides the repulsive force that allows the as-prepared surface to repel PDMS droplet in water. In addition, the outside surface of the PDMS droplet is coated with abundant hydrophobic $-CH_3$ groups which also have strong repellence to water (Figure 1e), so the PDMS droplet is difficult to replace the trapped water and penetrate into the laser-induced microstructures. Therefore, the underwater PDMS droplet sits on a composite (water/solid) interface and is at the underwater Cassie state (Figure 4d).[1,47−49] The PDMS droplet touches only a small area of the surface microstructures, and most area of the PDMS surface is surrounded by water. The hierarchical microstructure and the trapped water layer can effectively reduce the contact area, as well as van der Waals force, between the sample surface and the PDMS droplet, leading to a small adhesive force and adhesion of the laser-textured stainless steel surface to liquid polymer in water. So the laser-treated stainless steel surface shows underwater superpolymphobicity.

The underwater Cassie contact state of a PDMS droplet on the superpolymphobic multilevel microstructures in water can

DOI: 10.1021/acsanm.9b01869
ACS Appl. Nano Mater. 2019, 2, 7362−7371

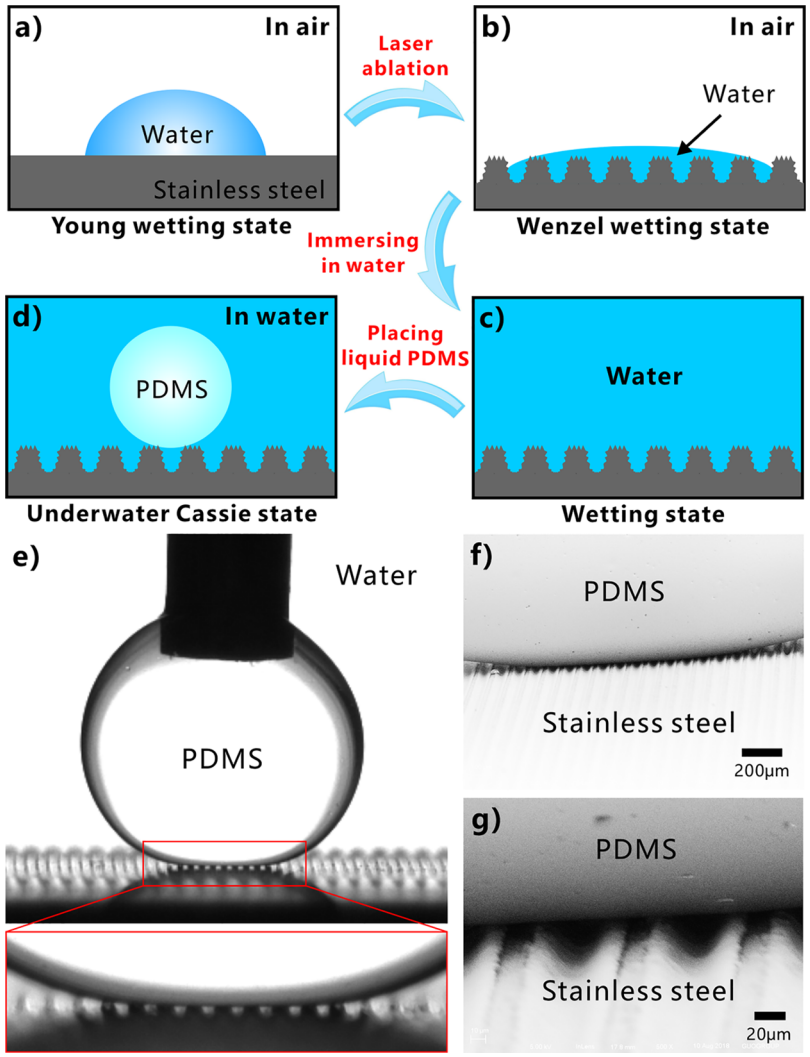

Figure 4. Formation mechanism of the laser-induced underwater superpolymphobicity on stainless steel surfaces. (a, b) Water droplets on (a) the untreated flat substrate and (b) the laser-induced hierarchical microstructure in air. (c) Immersion of the rough surface in water. (d) Underwater PDMS droplet on the rough microstructure. (e) Transmission optical photograph of the wetting between the microgroove-structured substrate and underwater liquid PDMS droplet, viewed along the direction of the microgrooves. (f, g) SEM images of the real wetting state of an underwater PDMS droplet on the microgroove-textured surface (after curing PDMS and removing water).

be directly verified by the transmission optical photograph and the SEM image. Figure 4e shows the enlarged image of an underwater PDMS droplet on the sample surface, viewed along the microgrooves direction. It is clear that there are sequential white light spots at the interface of the microgroove-textured substrate and liquid PDMS because background light can freely pass through this region. The light spots reveal that the underwater PDMS droplet just touches the peaks of the laser-induced microstructure and the space between stainless steel microstructure and PDMS droplet is filled with water (Figure 4d). Figure 4f,g is the SEM images which present the real contact state between the liquid PDMS droplet and the microgroove-textured surface in a water medium. The PDMS droplet was first cured at high temperature, and then the surrounding water was completely removed. It is found from the SEM images that the underwater PDMS droplet resides on the surface microstructure and is only in contact with the tips of the microstructure, affirming that PDMS is at the Cassie state on the rough stainless steel surface in water. With the regard of a polymer droplet on a rough substrate in water, the high PCA (θ^*_{PW}) accords with Cassie's equation:[1,36,41,50−53]

$$\cos\theta^*_{PW} = f(\cos\theta_{PW} + 1) - 1 \quad (1)$$

where f is the fraction of projected area of the polymer/substrate contact and θ_{PW} is the intrinsic PCA related to the polymer droplet on a flat substrate underwater. According to eq 1, the value of f can be inferred to be 0.15 (θ^*_{PW} = 156°, θ_{PW} = 116°). Such low f value indicates that the underwater PDMS droplet only contacts a small area of the rough surface, agreeing well with the observation results in Figure 4e−g. Multilevel microstructure has a stronger ability to capture water layer than the single-level structure; thereby the fs-laser-induced three-level microstructure is better for achieving underwater superpolymphobicity.

The interval of the laser scanning lines is controlled by the program during fs laser processing. Figure S3 shows the relationship between the surface wettability of the ablated stainless steel and the Λ. As the Λ increases, the super-hydrophilicity of the laser-ablated surface will gradually weaken (Figure S3a). The WCA of a water droplet on the sample surface increases with increasing Λ because the area fraction of the laser-treated region, as well as the average surface

DOI: 10.1021/acsanm.9b01869
ACS Appl. Nano Mater. 2019, 2, 7362−7371

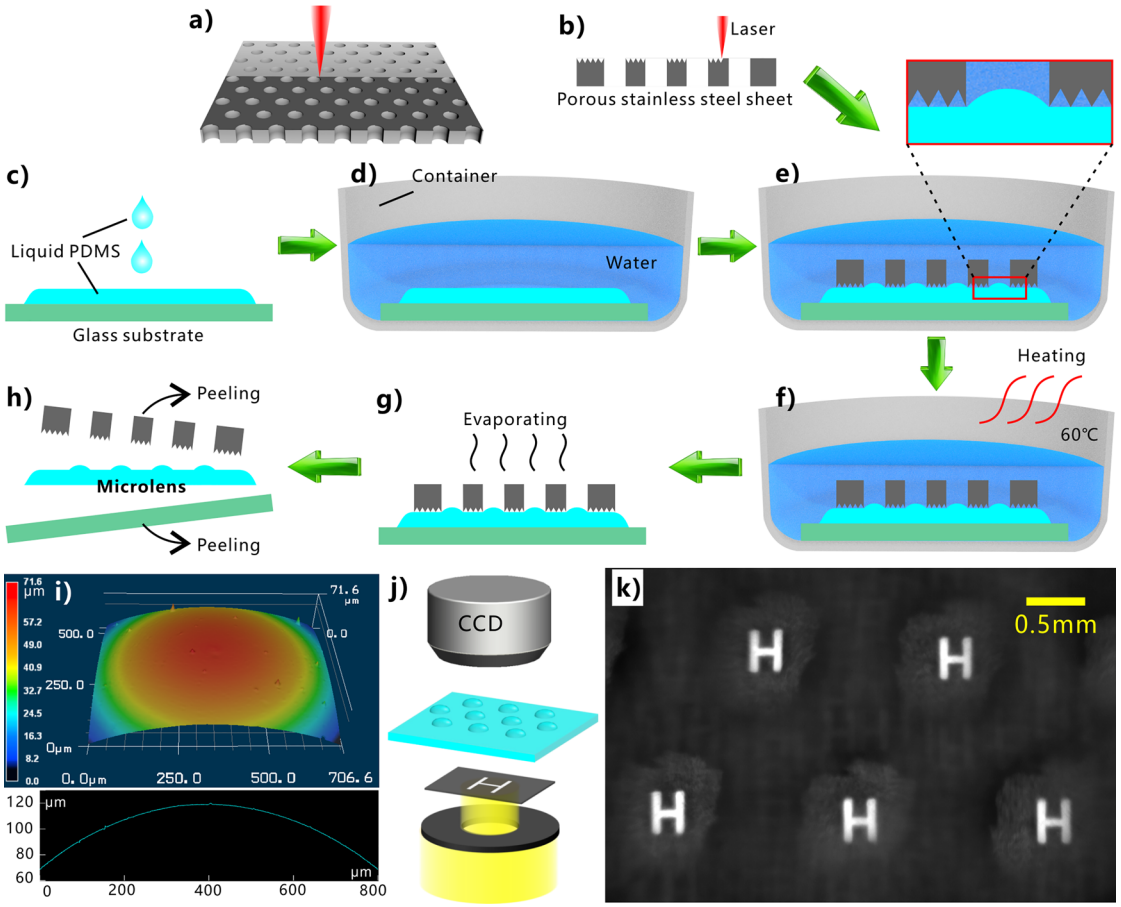

Figure 5. Preparation of microlens by using laser-induced underwater superpolymphobic surface. (a) Laser processing the stainless steel sheet with an array of through microholes. (b) Side view of ablating the porous sheet by laser. (c) Dropping PDMS liquid onto a glass substrate. (d) Shifting the glass substrate in a container and then being filled with water. (e) Placing the laser-processed metal sheet on the liquid PDMS layer. (f) Curing the PDMS liquid layer at 60 °C. (g) Removing the water environment. (h) Removing the porous metal sheet and the glass substrate from the PDMS sheet. (i) 3D morphology and profile of a single as-prepared microlens. (j) Simple optical system for the imaging measurement. (k) Imaging capacity of the microlens array.

roughness, declines. The water droplet usually spreads less on the laser-structured surface with larger Λ due to less wicking area. The superhydrophilicity was achieved when the Λ was no more than 140 μm, with the WCA values smaller than 10°. As shown in Figure S3b, the textured surface exhibits superpolymphobicity to underwater PDMS droplet with the Λ ranging from 60 to 200 μm, but the sample only has ultralow adhesion to the PDMS at $\Lambda \leq 180$ μm. The measured CAH of the PDMS droplet is no more than 4° on the sample surface with the Λ ranging from 60 to 180 μm. The CAH increases to $17 \pm 4°$ at $\Lambda = 200$ μm because the untreated area between the laser scanning lines is too large. As examples, Figure S3c,d depicts the dynamic underwater process of the suspended PDMS droplet contacting and leaving the sample surfaces fabricated at the Λ of 180 and 200 μm, respectively. The PDMS droplet was lowered slowly to contact the structured substrate, and then the droplet was controlled to leave the sample after appropriate contact. In the case of $\Lambda = 180$ μm, the PDMS droplet could depart from the substrate easily, without any residual adhering to the sample surface (Figure S3c). The PDMS droplet kept spherical shape during the whole contacting and leaving process, indicating the great PDMS repellence of the resultant surface. On the contrary, the PDMS droplet had an obvious shape deformation when it was just about to leave the surface with $\Lambda = 200$ μm (Figure S3d). The dynamic processes reveal that the as-prepared surfaces possessed ultralow adhesion to the PDMS droplet at $\Lambda = 180$ μm while exhibited higher adhesion to the PDMS droplet at $\Lambda = 200$ μm in water. Therefore, the ultralow adhesive superpolymphobicity can be easily obtained by the fs laser treatment with the $\Lambda \leq 180$ μm.

The superpolymphobicity of the laser-induced microstructure enables to control the shape of the liquid PDMS. Once the liquid PDMS is further cured at high temperature, the PDMS will solidify, and its shape will be fixed permanently. Figure 5 shows a proof-of-concept of preparing microlens array by using the underwater superpolymphobic microstructure. As a key optical component, microlens array is broadly applied in micro-optical systems, optical communication, adjusting light beam, high-definition displays, biochemical systems, photovoltaic devices, and artificial compound eyes.[54,55] A commercial porous stainless steel sheet (Figure S4a,b) was first ablated by laser to generate microstructures (Figure S4c,d) on its front surface (Figure 5a,b). The porous sheet with an array of through microholes (diameter = 0.8 mm) could be directly obtained from the metal market. On the other hand, liquid PDMS was dropped on a glass substrate (Figure 5c). The PDMS spread out and resulted in a liquid PDMS layer on the glass surface. The glass substrate was shifted to a container, and then water was slowly poured into the container (Figure 5d).

DOI: 10.1021/acsanm.9b01869
ACS Appl. Nano Mater. 2019, 2, 7362−7371

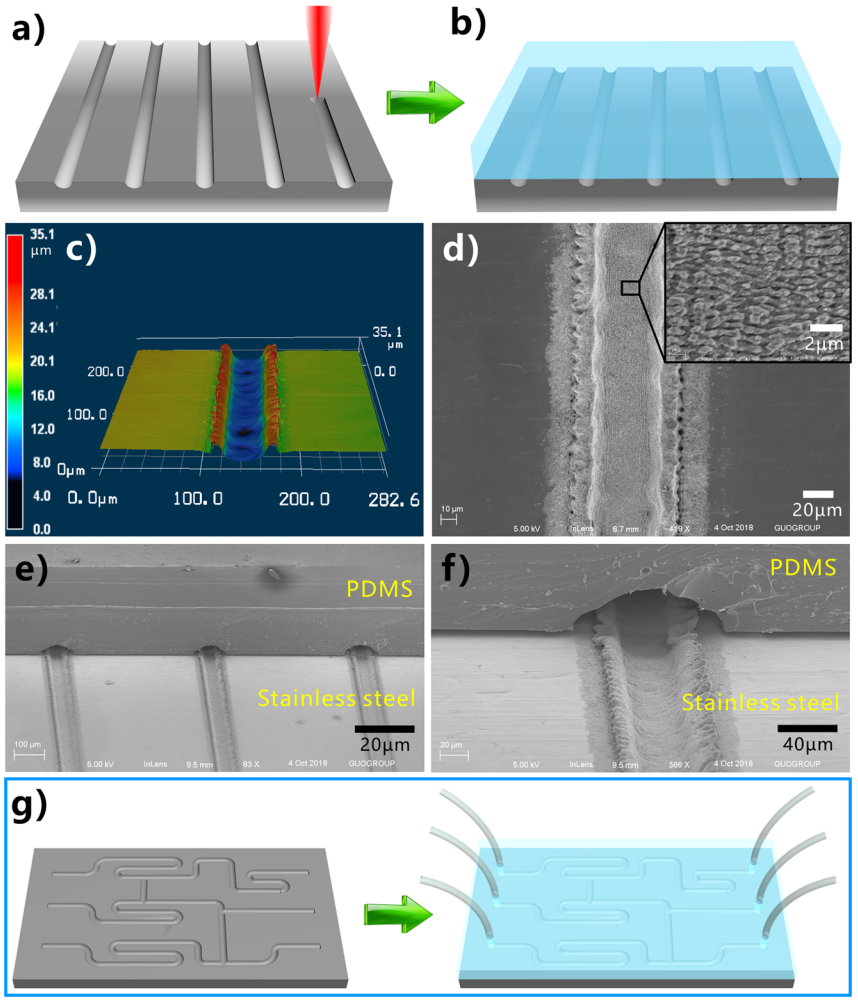

Figure 6. Preparation of microchannels system based on the laser-induced underwater superpolymphobic microgrooves. (a, b) Schematic of the fabrication of microchannels: (a) generating microgrooves on stainless steel substrate by laser direct writing, (b) microchannels system between stainless steel substrate and the cured PDMS coating. (c) 3D profile and (d) SEM image of a single microgroove that was generated from a single laser scanning line. The inset shows the high-magnification microstructure on the bottom of the microgroove. (e, f) SEM images of the cross-sectional view of the as-prepared microchannels. (g) Potential fabrication of a complex microfluids system.

Next, the laser-ablated porous stainless steel was placed onto the liquid PDMS layer, making the laser-treated side face the PDMS (Figure 5e). Because the contact between the liquid PDMS and the porous sheet was at the underwater Cassie state, the PDMS was unable to wet the surface of this porous sheet because of the laser-induced superpolymphobic microstructures. A convex meniscus of the PDMS/water interface was formed in every microhole of the porous sheet due to the surface tension and the press of the metal sheet (pressure ≈35.4 Pa), as shown in the inset of Figure 5e. The formation of such convex PDMS meniscus is ascribed to the surface tension which balances the pressure difference between two sides of the water/PDMS interface. After that, the PDMS was cured to solid state, which was performed by storing the water container at 60 °C for 3 h (Figure 5f). Next, the sandwich of porous metal sheet, solid PDMS sheet, and glass substrate was integrally taken out of water, allowing adhered water to evaporate completely (Figure 5g). Finally, the porous metal sheet and the glass substrate were easily peeled off from the PDMS sheet (Figure 5h). As a result, the PDMS sheet with an array of microscale convex meniscuses was obtained. Every solidified convex meniscus with good curved shape can act as a microlens with the radius of ∼1.6 mm and a focal length of ∼4.0 mm (Figure 5i).[56] The imaging capacity of the as-prepared microlens array was investigated by using a simple optical system, as shown in Figure 5j. A black thin sheet with a transparent letter "H" was used as the object, illuminated by a light beam. The microlens array was fixed on a movable stage between the object and a CCD camera. An array of bright images of "H" was clearly captured, with uniform size and shape (Figure 5k). The result reveals that the as-prepared PDMS microlens array has good imaging capacity. The diameter of the microlens depends on the size of the microholes on the porous sheet, while the height of the microlens can be adjusted by exerting a force (e.g., a weight) on the metal sheet during preparation.

The underwater superpolymphobic microstructure can also be used to prevent the adhesion at the PDMS/solid interface. As an example, we propose a method to fabricate microchannels which are the core component in the microfluidics. As the Λ is large enough, the laser-induced microgrooves are separated with each other, and the untreated flat domain exists between the microgrooves. First, microgrooves were created on the stainless steel surface by the fs laser direct writing (Figure 6a). The separated microgrooves had a width of ∼42.8 μm and depth of ∼17.5 μm (Figure 6c,d). A large number of

DOI: 10.1021/acsanm.9b01869
ACS Appl. Nano Mater. 2019, 2, 7362−7371

nanoripples coat on the bottom of the microgrooves (inset in Figure 6d). Following the same preparation process with the fabrication of microlens (without peeling off the cured PDMS layer), the microgrooves would develop to microchannels between the stainless steel and cured PDMS layer (Figure 6b). The underwater superpolymphobicity of the rough microstructures does not allow the liquid PDMS to enter into the laser-induced microgrooves; that is, the contact between the microgrooves and the liquid PDMS was effectively prevented. By contrast, the liquid PDMS could completely adhere to the nonablated domain. After curing the PDMS layer, the hollow microchannels formed between the stainless steel substrate and the cured PDMS layer, as shown in Figure 6e,f. It can be seen that the cured PDMS layer sickly adheres to the unablated domain while strides over the laser-induced microgrooves. The size of the as-prepared microchannel is mainly determined by the width/depth of the laser-induced microgrooves, which can be adjusted by laser power and scanning speed under fs laser treatment. Furthermore, laser-ablated track is programmable, so microgrooves with arbitrary shapes can be directly written by the fs laser, allowing us to potentially prepare various complex microfluidics systems (Figure 6g).

Although the underwater superpolymphobicity has a seemingly similar formation mechanism with the underwater superoleophobicity, they are two very different superwetting phenomena.[1] In comparison to oils, liquid polymers have complex composition, higher viscosity, and lower fluidity. More importantly, many liquid polymers (e.g., PDMS mixture) can be cured to solid state, thus enabling us to achieve a range of applications that have no resemblance to oil. In this work, we have demonstrated that the underwater superpolymphobicity has significant applications in control and design of the polymer shape and the polymer/substrate adhesion; none of these phenomena can find analogues in oil.

3. CONCLUSIONS

In conclusion, the phenomenon of repelling liquid polymer for a solid substrate in water was found. The stainless steel substrate was treated by fs laser processing to form three-level surface microstructures. After laser treatment, the whole surface was covered with nanoripples apart from the ablation-induced microgrooves and micromountains/microholes on the ridges. The liquid PDMS droplet shows the PCA of 156 ± 3° and CAH less than 4° on the laser-structured surface, demonstrating that the laser-induced microstructures have excellent underwater superpolymphobicity. The PDMS droplet on the superhydrophilic multilevel microstructures is at the Cassie contact state (underwater version), which was confirmed by the transmission optical photographs and the SEM images. In addition, we proposed a method to prepare microlens array by controlling the shape of the liquid PDMS before curing. The as-prepared microlens array exhibited well imaging capacity. A single laser scanning line finally develops into a microgroove which cannot bound with PDMS in water due to the superpolymphobicity, while the PDMS can adhere to the untreated area. Such selective adhesion was successfully applied to design microchannels in microfluidics system. We believe the underwater superpolymphobicity will have significant applications in designing and controlling the shape of the polymer materials and the adhesion between the polymers and a solid substrate.

4. EXPERIMENTAL SECTION

Materials. The flat stainless steel sheets and the porous stainless steel sheets were purchased from the local metal market. They were carefully cleaned by alcohol and water in this experiment. The liquid PDMS was the mixture of prepolymer and curing agent (DC-184, Dow Corning Corporation) with the volume proportion of 10:1. To cure the PDMS mixture, it was stored at 60 °C for 3 h.

Femtosecond Laser Treatment. As shown in Figure 1a, the stainless steel sheet was previously mounted on a translation platform controlled by a computer. The 67 fs laser pulses (center wavelength = 800 nm and repetition rate = 1 kHz) were focused onto the sample surface through a 250 mm focal-length plano-convex lens. Typical line-by-line scanning was adopted to ablate sample surface (Figure 1b).[27,28,49,57,58] The laser power and scanning speed were set constantly at 500 mW and 2.5 mm s^{-1}, respectively. The interval (Λ) of the laser scanning lines was controlled by the program. Finally, the ablated samples were cleaned with alcohol and distilled water.

Fabrication of the Microlens Array. The front surface of a commercial stainless steel sheet (25 × 25 × 0.75 mm^3, 2.22 g) with an array of through microholes (diameter = 0.8 mm) was first ablated by the fs laser to generate surface microstructures (Figure 5a,b). Meanwhile, liquid PDMS was poured onto a glass substrate to form a layer of liquid PDMS on the glass substrate (Figure 5c). The substrate was then shifted into a container, and water was slowly poured into the container (Figure 5d). Next, the laser-ablated porous stainless steel was placed onto the liquid PDMS layer, making the laser-treated side face the PDMS, as shown in Figure 5e. The curing and solidification of the liquid PDMS layer was performed by storing the water container at 60 °C for 3 h (Figure 5f). As a result, the liquid PDMS layer turned to a solid PDMS sheet. The glass substrate was taken out of the water container for further removing/evaporating all the adhered water (Figure 5g). After being peeled off the porous metal sheet and the glass substrate, a microlens array on the PDMS sheet was fabricated (Figure 5h).

Fabrication of Microchannels. First, microgrooves were generated on the stainless steel surface by fs laser scanning (Figure 6a). Meanwhile, the liquid PDMS was dropped on a glass substrate to form a layer of liquid PDMS on the glass substrate. The substrate was moved in a container, and water was slowly poured into the container. Next, the stainless steel sheet with microgrooves was placed onto the liquid PDMS layer, making the laser-treated side face the PDMS. The liquid PDMS layer was cured at 60 °C for 3 h, changing the PDMS from liquid state to solid state. Finally, the system including the glass substrate, the solid PDMS, and the metal sheet was took out of the water container and carefully peel off the glass substrate. So the microchannels were prepared between the stainless steel substrate and the cured PDMS layer, as shown in Figure 6b.

Characterization. The morphologies of the laser-structured stainless steel surface and the as-prepared microlens/microchannels were observed by a S-4100 scanning electron microscope (Hitachi, Japan) and a VK-9700 laser confocal microscope (Keyence, Japan). The wettabilities of water droplet and liquid PDMS droplet were characterized by using SL2000KB contact-angle measurement (Kino, America). Underwater wettability was measured by immersing the samples in a glass container filled with distilled water. The main volume of the water and PDMS droplets placed on stainless steel surfaces was ~10 μL, except that a smaller water droplet (3 μL) was dripped onto the textured surface for fully spreading.

■ ASSOCIATED CONTENT

Supporting Information

The Supporting Information is available free of charge on the ACS Publications website at DOI: 10.1021/acsanm.9b01869.

Cross-sectional profiles of the laser-induced microgrooves array at different location (Figure S1); underwater PDMS liquid droplet on the flat stainless steel surface (Figure S2); influence of the adopted interval of the laser scanning lines on the wettability of the laser-

DOI: 10.1021/acsanm.9b01869
ACS Appl. Nano Mater. 2019, 2, 7362−7371

ablated stainless steel surfaces (Figure S3); images of the porous stainless steel sheet before and after femtosecond laser ablation (Figure S4) (PDF)

Process of a small water droplet spreading out on the laser-induced rough surface in air (Movie S1) (AVI)

Process of an underwater liquid PDMS droplet being moved to contact and leave the rough stainless steel surface (Movie S2) (AVI)

AUTHOR INFORMATION

Corresponding Authors

*E-mail guo@optics.rochester.edu (C.G.).
*E-mail chenfeng@mail.xjtu.edu.cn (F.C.).

ORCID

Feng Chen: 0000-0002-7031-7404
Chunlei Guo: 0000-0001-8525-6301

Notes

The authors declare no competing financial interest.

ACKNOWLEDGMENTS

This work is supported by the Bill & Melinda Gates Foundation under Grant OPP1119542, the US Army Research Office under Grant W911NF1810204, and the National Key Research and Development Program of China under Grants 2017YFB1104700 and 2018YFB1107202.

REFERENCES

(1) Yong, J.; Chen, F.; Yang, Q.; Huo, J.; Hou, X. Superoleophobic Surface. *Chem. Soc. Rev.* **2017**, *46*, 4168−4217.
(2) Nishimoto, S.; Bhushan, B. Bioinspired Self-Cleaning Surfaces with Superhydrophobicity, Superoleophobicity, and Superhydrophilicity. *RSC Adv.* **2013**, *3*, 671−690.
(3) Ragesh, P.; Ganesh, V. A.; Nair, S. V.; Nair, A. S. A Review on 'Self-Cleaning and Multifunctional Materials'. *J. Mater. Chem. A* **2014**, *2*, 14773−14797.
(4) Lv, J.; Song, Y.; Jiang, L.; Wang, J. Bio-Inspired Strategies for Anti-Icing. *ACS Nano* **2014**, *8*, 3152−3169.
(5) Kreder, M. J.; Alvarenga, J.; Kim, P.; Aizenberg, J. Design of Anti-Icing Surfaces: Smooth, Textured or Slippery? *Nat. Rev. Mater.* **2016**, *1*, 1−15.
(6) Yong, J.; Chen, F.; Yang, Q.; Zhang, D.; Du, G.; Si, J.; Yun, F.; Hou, X. Femtosecond Laser Weaving Superhydrophobic Patterned PDMS Surfaces with Tunable Adhesion. *J. Phys. Chem. C* **2013**, *117*, 24907−24912.
(7) Wang, M.; Chen, C.; Ma, J.; Xu, J. Preparation of Superhydrophobic Cauliflower-Like Silica Nanospheres with Tunable Water Adhesion. *J. Mater. Chem.* **2011**, *21*, 6962−6967.
(8) Xue, Z.; Cao, Y.; Liu, N.; Feng, L.; Jiang, L. Special Wettable Materials for Oil/Water Separation. *J. Mater. Chem. A* **2014**, *2*, 2445−2460.
(9) Wang, B.; Liang, W.; Guo, Z.; Liu, W. Biomimetic Super-Lyophobic and Super-Lyophilic Materials Applied for Oil/Water Separation: A New Strategy Beyond Nature. *Chem. Soc. Rev.* **2015**, *44*, 336−361.
(10) Yong, J.; Huo, J.; Chen, F.; Yang, Q.; Hou, X. Oil/Water Separation Based on Natural Materials with Super-Wettability: Recent Advances. *Phys. Chem. Chem. Phys.* **2018**, *20*, 25140−25163.
(11) Genzer, J.; Efimenko, K. Recent Developments in Superhydrophobic Surfaces and Their Relevance to Marine Fouling: A Review. *Biofouling* **2006**, *22*, 339−360.
(12) Pan, S.; Kota, A. K.; Mabry, J. M.; Tuteja, A. Superomniphobic Surfaces for Effective Chemical Shielding. *J. Am. Chem. Soc.* **2013**, *135*, 578−581.
(13) Shi, F.; Niu, J.; Liu, J.; Liu, F.; Wang, Z.; Feng, X.; Zhang, X. Towards Understanding Why a Superhydrophobic Coating Is Needed by Water Striders. *Adv. Mater.* **2007**, *19*, 2257−2261.
(14) Vitale, A.; Quaglio, M.; Marasso, S. L.; Chiodoni, A.; Cocuzza, M.; Bongiovanni, R. Direct Photolithography of Perfluoropolyethers for Solvent-Resistant Microfluidics. *Langmuir* **2013**, *29*, 15711−15718.
(15) Kwon, K. W.; Choi, S. S.; Lee, S. H.; Kim, B.; Lee, S. N.; Park, M. C.; Kim, P.; Hwang, S. Y.; Suh, K. Y. Label-Free, Microfluidic Separation and Enrichment of Human Breast Cancer Cells by Adhesion Difference. *Lab Chip* **2007**, *7*, 1461−1468.
(16) Stratakis, E.; Ranella, A.; Fotakis, C. Biomimetic Micro/Nanostructured Functional Surfaces for Microfluidic and Tissue Engineering Applications. *Biomicrofluidics* **2011**, *5*, 013411.
(17) Shen, L.; Wang, B.; Wang, J.; Fu, J.; Picart, C.; Ji, J. Asymmetric Free-Standing Film with Multifunctional Anti-Bacterial and Self-Cleaning Properties. *ACS Appl. Mater. Interfaces* **2012**, *4*, 4476−4483.
(18) Zhang, S.; Huang, J.; Chen, Z.; Lai, Y. Bioinspired Special Wettability Surfaces: From Fundamental Research to Water Harvesting Applications. *Small* **2017**, *13*, 1602992.
(19) Wang, S.; Wang, T.; Ge, P.; Xue, P.; Ye, S.; Chen, H.; Li, Z.; Zhang, J.; Yang, B. Controlling Flow Behavior of Water in Microfluidics with a Chemically Patterned Anisotropic Wetting Surface. *Langmuir* **2015**, *31*, 4032−4039.
(20) Songok, J.; Tuominen, M.; Teisala, H.; Haapanen, J.; Mäkelä, J.; Kuusipalo, J.; Toivakka, M. Paper-Based Microfluidics: Fabrication Technique and Dynamics of Capillary-Driven Surface Flow. *ACS Appl. Mater. Interfaces* **2014**, *6*, 20060−20066.
(21) Yong, J.; Yang, Q.; Chen, F.; Zhang, D.; Du, G.; Si, J.; Yun, F.; Hou, X. A Bioinspired Planar Superhydrophobic Microboat. *J. Micromech. Microeng.* **2014**, *24*, 035006.
(22) Jokinen, V.; Sainiemi, L.; Franssila, S. Complex Droplets on Chemically Modified Silicon Nanograss. *Adv. Mater.* **2008**, *20*, 3453−3456.
(23) Wen, L.; Tian, Y.; Jiang, L. Bioinspired Super-Wettability from Fundamental Research to Practical Applications. *Angew. Chem., Int. Ed.* **2015**, *54*, 3387−3399.
(24) Tian, Y.; Su, B.; Jiang, L. Interfacial Material System Exhibiting Superwettability. *Adv. Mater.* **2014**, *26*, 6872−6897.
(25) Liu, M.; Wang, S.; Jiang, L. Nature-Inspired Superwettability Systems. *Nat. Rev. Mater.* **2017**, *2*, 17036.
(26) Su, B.; Tian, Y.; Jiang, L. Bioinspired Interfaces with Superwettability: From Materials to Chemistry. *J. Am. Chem. Soc.* **2016**, *138*, 1727−1748.
(27) Yong, J.; Yang, Q.; Chen, F.; Zhang, D.; Farooq, U.; Du, G.; Hou, X. A Simple Way to Achieve Superhydrophobicity, Controllable Water Adhesion, Anisotropic Sliding, and Anisotropic Wetting Based on Femtosecond-Laser-Induced Line-Patterned Surfaces. *J. Mater. Chem. A* **2014**, *2*, 5499−5507.
(28) Yong, J.; Chen, F.; Li, M.; Yang, Q.; Fang, Y.; Huo, J.; Hou, X. Remarkably Simple Achievement of Superhydrophobicity, Superhydrophilicity, Underwater Superoleophobicity, Underwater Superoleophilicity, Underwater Superaerophobicity, and Underwater Superaerophilicity on Femtosecond Laser Ablated PDMS Surfaces. *J. Mater. Chem. A* **2017**, *5*, 25249−25257.
(29) Marmur, A. Hydro- Hygro- Oleo- Omni-Phobic? Terminology of Wettability Classification. *Soft Matter* **2012**, *8*, 6867−6870.
(30) Baldacchini, T.; Carey, J. E.; Zhou, M.; Mazur, E. Superhydrophobic Surfaces Prepared by Microstructuring of Silicon Using a Femtosecond Laser. *Langmuir* **2006**, *22*, 4917−4919.
(31) Zorba, V.; Stratakis, E.; Barberoglou, M.; Spanakis, E.; Tzanetakis, P.; Anastasiadis, S. H.; Fotakis, C. Biomimetic Artificial Surfaces Quantitatively Reproduce the Water Repellency of a Lotus Leaf. *Adv. Mater.* **2008**, *20*, 4049−4054.
(32) Chen, F.; Zhang, D.; Yang, Q.; Wang, X.; Dai, B.; Li, X.; Hao, X.; Ding, Y.; Si, J.; Hou, X. Anisotropic Wetting on Microstrips Surface Fabricated by Femtosecond Laser. *Langmuir* **2011**, *27*, 359−365.

DOI: 10.1021/acsanm.9b01869
ACS Appl. Nano Mater. 2019, 2, 7362−7371

(33) Zhang, D.; Chen, F.; Yang, Q.; Si, J.; Hou, X. Mutual Wetting Transition between Isotropic and Anisotropic on Directional Structures Fabricated by Femotosecond Laser. *Soft Matter* **2011**, *7*, 8337−8342.
(34) Zhang, D.; Chen, F.; Yang, Q.; Yong, J.; Bian, H.; Ou, Y.; Si, J.; Meng, X.; Hou, X. A Simple Way To Achieve Pattern-Dependent Tunable Adhesion in Superhydrophobic Surfaces by a Femtosecond Laser. *ACS Appl. Mater. Interfaces* **2012**, *4*, 4905−4912.
(35) Yong, J.; Yang, Q.; Chen, F.; Zhang, D.; Bian, H.; Ou, Y.; Si, J.; Du, G.; Hou, X. Stable Superhydrophobic Surface with Hierarchical Mesh-Porous Structure Fabricated by a Femtosecond Laser. *Appl. Phys. A: Mater. Sci. Process.* **2013**, *111*, 243−249.
(36) Yong, J.; Chen, F.; Yang, Q.; Zhang, D.; Farooq, U.; Du, G.; Hou, X. Bioinspired Underwater Superoleophobic Surface with Ultralow Oil-Adhesion Achieved by Femtosecond Laser Microfabrication. *J. Mater. Chem. A* **2014**, *2*, 8790−8795.
(37) Yong, J.; Chen, F.; Fang, Y.; Huo, J.; Yang, Q.; Zhang, J.; Bian, H.; Hou, X. Bioinspired Design of Underwater Superaerophobic and Superaerophilic Surfaces by Femtosecond Laser Ablation for Anti- or Capturing Bubbles. *ACS Appl. Mater. Interfaces* **2017**, *9*, 39863−39871.
(38) Yong, J.; Chen, F.; Yang, Q.; Fang, Y.; Huo, J.; Zhang, J.; Hou, X. Nepenthes Inspired Design of Self-Repairing Omniphobic Slippery Liquid Infused Porous Surface (SLIPS) by Femtosecond Laser Direct Writing. *Adv. Mater. Interfaces* **2017**, *4*, 1700552.
(39) Yong, J.; Huo, J.; Yang, Q.; Chen, F.; Fang, Y.; Wu, X.; Liu, L.; Lu, X.; Zhang, J.; Hou, X. Femtosecond Laser Direct Writing of Porous Network Microstructures for Fabricating Super-Slippery Surfaces with Excellent Liquid Repellence and Anti-Cell Proliferation. *Adv. Mater. Interfaces* **2018**, *5*, 1701479.
(40) Feng, L.; Li, S.; Li, Y.; Li, H.; Zhang, L.; Zhai, J.; Song, Y.; Liu, B.; Jiang, L.; Zhu, D. Super-Hydrophobic Surfaces: From Natural to Artificial. *Adv. Mater.* **2002**, *14*, 1857−1860.
(41) Liu, M.; Wang, S.; Wei, Z.; Song, Y.; Jiang, L. Bioinspired Design of a Superoleophobic and Low Adhesive Water/Solid Interface. *Adv. Mater.* **2009**, *21*, 665−669.
(42) Sugioka, K.; Cheng, Y. Femtosecond Laser Three-Dimensional Micro- and Nanofabrication. *Appl. Phys. Rev.* **2014**, *1*, 041303.
(43) Wu, B.; Zhou, M.; Li, J.; Ye, X.; Li, G.; Cai, L. Superhydrophobic Surfaces Fabricated by Microstructuring of Stainless Steel Using a Femtosecond Laser. *Appl. Surf. Sci.* **2009**, *256*, 61−66.
(44) Vorobyev, A. V.; Guo, C. Metal Pumps Liquid Uphill. *Appl. Phys. Lett.* **2009**, *94*, 224102.
(45) Vorobyev, A. Y.; Guo, C. Laser Turns Silicon Superwicking. *Opt. Express* **2010**, *18*, 6455−6460.
(46) Vorobyev, A. Y.; Guo, C. WaterSprints Uphill on Glass. *J. Appl. Phys.* **2010**, *108*, 123512.
(47) Yong, J.; Singh, S. C.; Zhan, Z.; Chen, F.; Guo, C. Substrate-Independent, Fast, and Reversible Switching between Underwater Superaerophobicity and Aerophilicity on the Femtosecond Laser-Induced Superhydrophobic Surfaces for Selectively Repelling or Capturing Bubbles in Water. *ACS Appl. Mater. Interfaces* **2019**, *11*, 8667−8675.
(48) Yong, J.; Singh, S. C.; Zhan, Z.; Chen, F.; Guo, C. How To Obtain Six Different Superwettabilities on a Same Microstructured Pattern: Relationship between Various Superwettabilities in Different Solid/Liquid/Gas Systems. *Langmuir* **2019**, *35*, 921−927.
(49) Yong, J.; Singh, S. C.; Zhan, Z.; Huo, J.; Chen, F.; Guo, C. Reducing Adhesion for Dispensing Tiny Water/Oil Droplets and Gas Bubbles by Femtosecond Laser-Treated Needle Nozzles: Superhydrophobicity, Superoleophobicity, and Superaerophobicity. *ChemNanoMat* **2019**, *5*, 241−249.
(50) Jung, Y. C.; Bhushan, B. Wetting Behavior of Water and Oil Droplets in Three-Phase Interfaces for Hydrophobicity/philicity and Oleophobicity/philicity. *Langmuir* **2009**, *25*, 14165−14173.
(51) Jung, Y. C.; Bhushan, B. Dynamic Effects Induced Transition of Droplets on Biomimetic Superhydrophobic Surfaces. *Langmuir* **2009**, *25*, 9208−9218.
(52) Jung, Y. C.; Bhushan, B. Mechanically Durable Carbon Nanotube Composite Hierarchical Structures with Superhydrophobicity, Self-Cleaning, and Low-Drag. *ACS Nano* **2009**, *3*, 4155−4163.
(53) Bhushan, B.; Jung, Y. C.; Koch, K. Micro-, Nano- and Hierarchical Structures for Superhydrophobicity, Self-Cleaning and Low Adhesion. *Philos. Trans. R. Soc., A* **2009**, *367*, 1631−1672.
(54) Sun, Y.-L.; Dong, W.-F.; Yang, R.-Z.; Meng, X.; Zhang, L.; Chen, Q.-D.; Sun, H.-B. Dynamically Tunable Protein Microlenses. *Angew. Chem., Int. Ed.* **2012**, *51*, 1558−1562.
(55) Li, X.; Ding, Y.; Shao, J.; Tian, H.; Liu, H. Fabrication of Microlens Arrays with Well-Controlled Curvature by Liquid Trapping and Electrohydrodynamic Deformation on Microholes. *Adv. Mater.* **2012**, *24*, OP165−OP169.
(56) Yong, J.; Chen, F.; Yang, Q.; Du, G.; Bian, H.; Zhang, D.; Si, J.; Yun, F.; Hou, X. Rapid Fabrication of Large-Area Concave Microlens Arrays on PDMS by a Femtosecond Laser. *ACS Appl. Mater. Interfaces* **2013**, *5*, 9382−9385.
(57) Yong, J.; Yang, Q.; Guo, C.; Chen, F.; Hou, X. A Review of Femtosecond Laser-Structured Superhydrophobic or Underwater Superoleophobic Porous Surfaces/Materials for Efficient Oil/Water Separation. *RSC Adv.* **2019**, *9*, 12470−12495.
(58) Bai, X.; Yang, Q.; Fang, Y.; Zhang, J.; Yong, J.; Hou, X.; Chen, F. Superhydrophobicity-Memory Surfaces Prepared by a Femtosecond Laser. *Chem. Eng. J.* **2019**, 123143.

DOI: 10.1021/acsanm.9b01869
ACS Appl. Nano Mater. 2019, 2, 7362−7371